Molecular Vision 2006; 12:32-42 <http://www.molvis.org/molvis/v12/a4/>
Received 22 July 2005 | Accepted 5 January 2006 | Published 12 January 2006

Effects of VEGFR-1, VEGFR-2, and IGF-IR hammerhead ribozymes on glucose-mediated tight junction expression in cultured human retinal endothelial cells

Polyxenie E. Spoerri,[1] Aqeela Afzal,[1] Sergio Li Calzi,[1] Lynn C. Shaw,[1] Jun Cai,[2] Hao Pan,[1] Michael Boulton,[2] Maria B. Grant[1]

[1]Department of Pharmacology and Therapeutics, College of Medicine, University of Florida, Gainesville, FL; [2]School of Optometry and Vision Sciences, Cardiff University, Cardiff, UK

Purpose: To evaluate whether transfection of human retinal endothelial cells (HRECs) with plasmids expressing ribozymes designed to specifically cleave the mRNA and reduce expression of either vascular endothelial growth factor (VEGF) receptor-1 (VEGFR-1), or VEGF receptor-2 (VEGFR-2), or insulin-like growth factor-I receptor (IGF-IR) modulates occludin expression in high glucose-treated cells.

Methods: Hammerhead ribozymes that specifically cleave the human VEGFR-1, VEGFR-2, and IGF-IR mRNAs were developed and tested in vitro to determine ribozyme kinetics and cleavage specificity. HRECs grown in normal (5.5 mM) and high (25 mM) glucose medium were transfected with plasmids expressing VEGFR-1, VEGFR-2, or IGF-IR hammerhead ribozymes. VEGF and IGF-I levels were measured in conditioned medium of HREC exposed to high glucose conditions, and the effect of varying glucose concentration on VEGFR-1 and VEGFR-2 phosphorylation was examined. The amount of the tight junction protein occludin was determined by western analysis, and the protein was localized by immunohistochemistry.

Results: Exposure of HRECs to high glucose resulted in increased VEGF and IGF-I expression as well as VEGFR-2 but not VEGFR-1 phosphorylation. Immunocytochemistry and western analysis revealed that HRECs exposed to high glucose had reduced occludin staining and protein expression, respectively. Transfection of HRECs exposed to high glucose with either VEGFR-1, VEGFR-2, or IGF-IR hammerhead ribozymes prevented the downregulation of occludin protein expression.

Conclusions: Our studies support that activation of VEGFR-1, VEGFR-2, and IGF-IR by high glucose contributes to disruption of tight junctions by decreasing occludin expression and may be important in the pathogenesis of blood-retinal barrier dysfunction in diabetic retinopathy.

Chronic hyperglycemia in diabetes is associated with the development and progression of pathological changes in the retinal vasculature involving breakdown of the blood-retinal barrier (BRB) [1,2]. The endothelium forms the BRB in retinal capillary vessels and its permeability is regulated by tight junctions between adjacent endothelial cells [3]. Occludin and claudins span the plasma membrane and limit flow of vascular fluids between endothelial cells, while other proteins, zonula occludens-1, 2, 3 (ZO-1, 2, 3), symplekin, 7H6, and cingulin are tight junction-associated proteins that reside in the peripheral cytoplasm and organize the junction [4]. Occludin, a 65 kDa transmembrane protein of the tight junction, is primarily responsible for forming the permeability barrier [5,6].

A study involving streptozotocin-induced diabetic rats showed a reduced quantity of occludin at the tight junctions of endothelial cells in retinal arterioles and capillaries [7]. Furthermore, three months of streptozotocin-induced diabetes in rats caused an increase in retinal permeability to albumin. In the same study, treatment of bovine retinal endothelial cell cultures (BRECs) with vascular endothelial growth factor (VEGF) caused a similar decrease in occludin [8]. Moreover, streptozotocin-induced diabetes or VEGF treatment increased paracellullar vascular permeability in the rat retina and was associated with redistribution of occludin [9].

The early stages of vascular dysfunction in diabetes involve a permeability defect of the retinal vasculature and correlate with increases in expression of VEGF [10-12]. VEGF exerts its functions on endothelial cells via interaction with cellular receptors, VEGFR-1 and VEGFR-2 [13-15]. It is generally considered that activation of VEGFR-1 regulates the metabolism of a range of vascular and nonvascular cells, while activation of VEGFR-2 promotes cell migration and proliferation of endothelial cells [16]. Some studies have suggested that VEGFR-2 is the receptor responsible for the permeability activity [17,18]. However, a mutant form of VEGF that lacks VEGFR-2 activation retained the ability to induce permeability [19], suggesting that changes in permeability may be mediated by a receptor other than VEGFR-2.

Other cytokines, in particular insulin-like growth factor-I (IGF-I), may be involved in retinal vascular permeability [20]. Altered serum IGF-I levels may be clinically meaningful in both type 1 [21] and type 2 diabetes [22,23] associated with macular edema [24,25]. Brausewetter and coworkers con-

Correspondence to: Maria B. Grant, 1600 SW Archer Road, Box 100267, Gainesville, FL, 32610; Phone: (352) 846-0978; FAX: (352) 392-9696; email: grantma@pharmacology.ufl.edu

cluded that capillary permeability is increased in both types of diabetes mellitus, and that IGF-I is a key mediator affecting microvascular permeability [26].

Local tissue levels of IGF-I may be even more relevant than serum levels to the initiation of vascular pathology including changes in permeability. We and others have demonstrated an increase of IGF-I in the vitreous of diabetics with PDR compared to nondiabetic individuals and levels correlated with severity of macular edema and preretinal neovascularization [27-29]. Furthermore, intravitreal injection of high levels of IGF-I results in the breakdown of the BRB and neovascularization in pig [30] and rabbit [31] models.

IGF-I has been shown to increase VEGF gene expression, regulate VEGF-dependent retinal neovascularization, and act as an indirect angiogenic factor in animal models of retinal ischemia [32]. IGF-IR has been shown to regulate VEGF action through control of VEGF activation of p44/42 mitogen-activated protein kinase (MAPK), establishing a hierarchical relationship between IGF-IR and VEGF receptors [33]. The converse is also true in that VEGF induces IGF-I expression in HREC [34].

For the current studies, we synthesized and tested hammerhead ribozymes that specifically cleave VEGFR-1, VEGFR-2, and IGF-IR mRNAs, respectively [35]. Ribozymes are catalytic RNA molecules that cleave phosphodiester bonds between RNA nucleotides [36]. Two types of ribozymes that are based on self-cleaving viral agents, hairpins and hammerheads, have been used as potential gene therapy agents. Hammerhead ribozymes have been used more commonly because they have a greater range of target sites [37]. Previously, we demonstrated the efficacy of this IGF-IR ribozyme to reduce IGF-I receptor protein and function [28].

In this study, we validated the specificity of the VEGFR-1 and VEGFR-2 ribozymes for their respective targets, characterized the effect of VEGF receptor reduction on IGF-I receptor levels, and determined the effect of IGF-I receptor reduction on VEGF receptor levels.

We also investigated the effect of high glucose (25 mM) on VEGF-1 and IGF-I protein expression, VEGFR-1 and VEGFR-2 phosphorylation, and occludin protein expression in cultured retinal endothelial cells (RECs). Finally, we evaluated whether transfection with these ribozymes modulate the effect of glucose on occludin expression.

METHODS

Synthetic RNA targets and ribozymes: RNA oligonucleotides for the hammerhead ribozymes and targets were purchased from Dharmacon (Boulder, CO) and deprotected following the manufacturer's protocol. RNA oligonucleotides were 5'-end labeled with [γ-^{32}P]-dATP (ICN, Irving, CA) using polynucleotide kinase (Promega, Madison, WI).

Time course analysis of ribozyme cleavage: Time course analysis of cleavage was performed using the RNA oligonucleotides as described elsewhere [35,38]. For each reaction two picomoles of ribozyme (15 nM final) in 40 mM Tris-HCl, pH 7.5 was incubated at 65 °C for 2 min then incubated at 25 °C for 10 min. Dithiotheritol (DTT, 20 mM final), RNasin (4 units, Promega), and $MgCl_2$ (20 mM final) were added, and the mixture was incubated at 37 °C for 10 min. Cleavage was initiated by the addition of the ^{32}P-end labeled target RNA oligonucleotide, and the reaction proceeded at 37 °C. Variations on this protocol include incubation at 25 °C at 1, 5, 10, and 20 mM $MgCl_2$. Aliquots were removed at various times and added to an equal volume of formamide stop buffer (90% formamide, 50 mM EDTA, 0.05% bromophenol blue, 0.05% xylene cyanol) and held on ice. The samples were then heat denatured at 95 °C for 2 min, placed on ice and the reaction products were separated on 10% polyacrylamide-8M urea gels. The gels were analyzed on a Molecular Dynamics PhosphoImager.

Cloning of the hammerhead ribozymes into the rAAV vector: To produce a double-stranded DNA fragment coding for each hammerhead ribozyme, two complementary DNA oligonucleotides (Life Technologies, Gaithersburg, MD) were annealed. All DNA oligonucleotides were synthesized with 5'-phosphate groups. The DNA oligonucleotides were designed to generate a cut HindIII site at the 5' end and a cut SpeI site at the 3' end after annealing. The DNA oligonucleotides were incubated at 65 °C for 2 min and annealed by slow cooling to room temperature for 30 min. The resulting double-stranded DNA fragment was ligated into the HindIII and SpeI sites of the recombinant adeno-associated viral vector p21NewHp [39]. The ligated plasmids were transformed into SURE electroporation competent cells (Stratagene, La Jolla, CA) in order to maintain the integrity of the inverted terminal repeats. The ribozyme clones were verified by sequencing.

Time course of cleavage analysis of hammerhead ribozymes: Time course of cleavage analysis was carried out as previously described [39,40]. RNA oligonucleotides representing the VEGFR-1, VEGFR-2, and IGF-IR ribozymes (34 nucleotides) and targets (13 nucleotides) were purchased from Dharmacon. Cleavage reactions were carried out at 37 °C and in 20 mM $MgCl_2$ at a 1:10 M ratio of ribozyme:target. Target oligonucleotides were 5'-end labeled with α-^{32}P-ATP and products of cleavage were separated on 10% polyacrylamide-8M urea gels and analyzed on a Molecular Dynamics PhosphorImager (Model Storm 820, GE Healthcare, Fairfield, CT).

Human retinal endothelial cell culture: Human eyes from six donors were obtained from the National Disease Research Interchange within 36 h of death. Human retinal endothelial cells (HRECs) were prepared and maintained as previously described [41]. The identity of HRECs was validated by demonstrating endothelial cell incorporation of fluorescence-labeled, acetylated LDL, and by fluorescence-activated cell-sorting analysis, as previously described [41]. Cells in passages 3 to 5 were used in the studies [42]. To determine the effect of high glucose, HRECs were grown for 7 days in normal (5.5 mM) or high (25 mM) D-glucose medium.

Bovine retinal endothelial cell culture: BRECs were isolated as previously described [43]. In brief, isolated bovine retinas in ice cold Eagle's minimal essential medium (MEM) with HEPES were homogenized by a Teflon-glass homogenizer and microvessels trapped on an 83 mm nylon mesh.

Vessels were transferred into 2X MEM containing 500 μg/ml collagenase, 200 μg/ml pronase (BDH, Poole, UK) and 200 μg/ml DNase at 37 °C for 20 min. The resultant vessel fragments were trapped on 53 μm mesh, washed with cold MEM, and centrifuged at 225x g for 10 min. The pellet was suspended in microvascular endothelial cell basal medium (MECBM) with growth supplement (TCS Works Ltd., Buckingham, UK) at 37 °C, 5% CO_2 for 3 days. Confluent cells were used between passages 1 and 3.

Transfection of HRECs with Lipofectamine: HRECs grown to confluence on 150 mm plates in normal and high glucose medium were transfected with the VEGFR-1, VEGFR-2, and IGF-IR ribozyme plasmid constructs using Lipofectamine 2000 as described elsewhere [44]. Opti-MEM I (728 μl) was combined with Lipofectamine 2000 (52 μl, Invitrogen, Carlsbad, CA) and kept at room temperature for 5 min. Then, 780 μl of Opti-MEM I was combined with 13 μg of DNA and allowed to sit at room temperature for 5 min. These two solutions were then combined and complexed for 20 min at room temperature. While the solutions were complexing, the cultures were removed from the incubator and the medium from each petri dish was aspirated and replaced with fresh medium without antibiotics. These plates were then returned to the incubator until the time of addition of the complexes. After 20 min of complexing the Opti-MEM I/DNA/Lipofectamine 2000 was added to the cultures at 1560 μl per petri dish. The culture medium was replaced after 24 h. The cells were harvested after 72 h of incubation for further analysis.

Reverse transcription: Total RNA was extracted from HRECs using Trizol reagent (Invitrogen) according to manufacturer's protocol. For each reverse transcription reaction 4 μg of total RNA was reverse transcribed using iScript™ cDNA synthesis Kit (BioRad, Hercules, CA) according to the manufacturer's protocol.

Real-time PCR: Real-time PCR was performed on 4 μl of the cDNA reverse transcription product using iQ™ SYBR Green Supermix (BioRad) according to the manufacturer's protocol. Primer pairs for VEGFR-1 and VEGFR-2 (R & D Systems, Minneapolis, MN) were used at 7.5 nM. All reac-

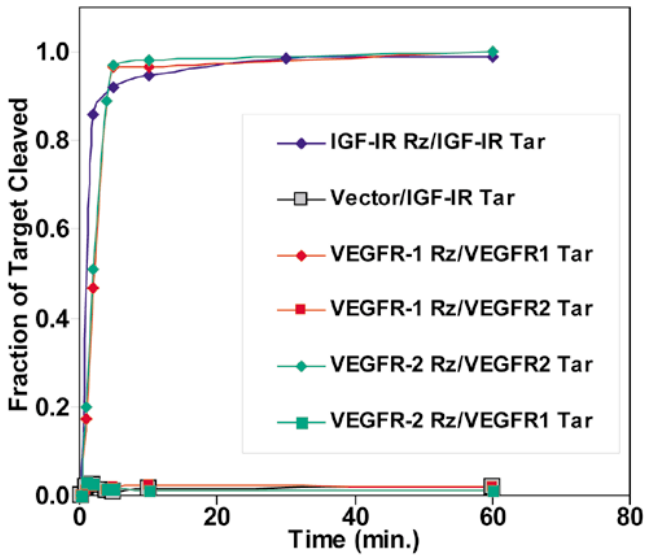

Figure 1. All three ribozymes have similar catalytic activity. Time course of cleavage analysis for VEGFR-1, VEGFR-2, and IGF-IR ribozymes (Rz) on 13-nucleotide synthetic RNA targets (Tar) demonstrates that the catalytic activities of the ribozymes are similar. In addition, this graph demonstrates the specificity of the VEGFR-1 and VEGFR-2 for their respective targets.

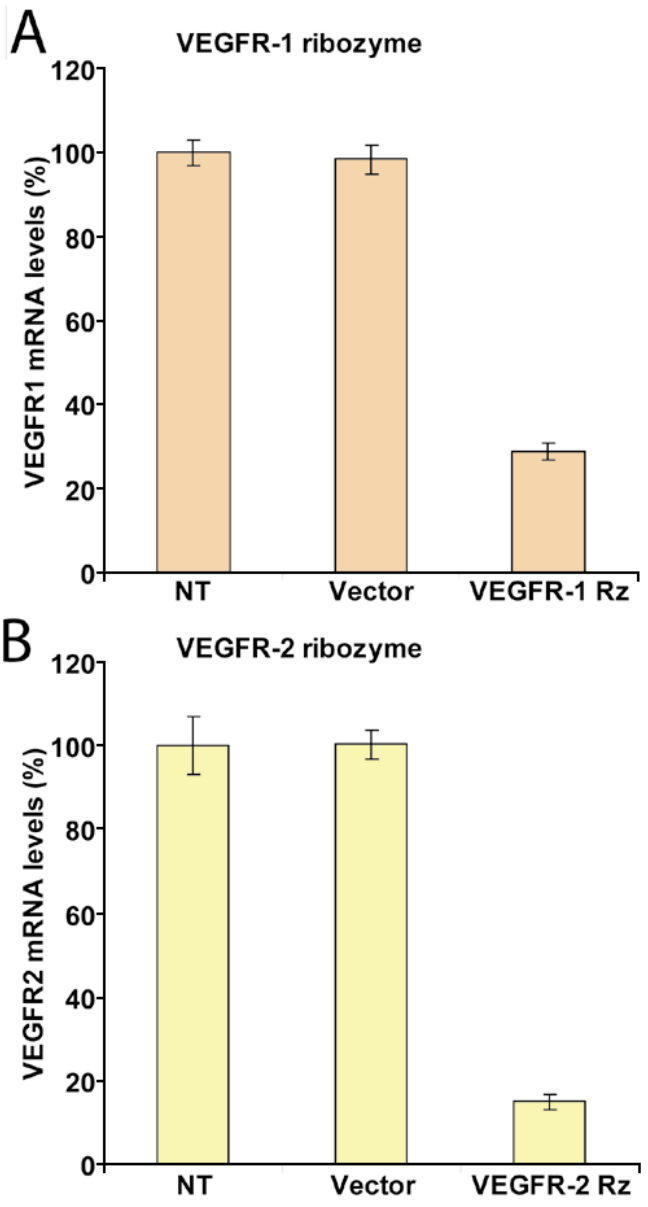

Figure 2. VEGFR-1 and VEGFR-2 mRNA expression is inhibited by the ribozymes. The VEGFR-1 (**A**) and VEGFR-2 (**B**) ribozymes specifically reduce levels of their respective target mRNAs. The graph shows the results of real-time PCR on cDNAs produced from total RNA isolated from nontransfected (NT) human retinal endothelial cells (HRECs), from HRECs transfected with plasmids expressing the VEGFR-1 (VEGFR-1 Rz) or VEGFR-2 (VEGFR-2 Rz) ribozymes. For each sample the level of the VEGFR-1 or VEGFR-2 mRNA was determined relative to β-actin mRNA.

tions were performed in duplicate using positive control cDNA (R & D Systems). Samples were normalized to β-actin (Ambion, Austin, TX). Real-time PCR was performed on a DNA engine Opticon system with continuous fluorescence detector (MJ Research, Waltham, MA). Thermal cycler conditions were denaturation at 94 °C for 1 min, annealing at 55 °C for 1 min, elongation at 72 °C for 1 min, for 60 cycles. Opticon Monitor analysis software (MJ Research, Waltham, MA) was used for analysis.

ELISA for VEGF: VEGF protein concentration was determined from HREC-conditioned medium using the Quantikine® Human VEGF Immunoassay ELISA kit (R & D Systems). HREC were treated with either 5.5 or 25 mM glucose and aliquots were taken daily for analysis.

ELISA for IGF-I: IGF-I protein concentration was determined from HREC-conditioned medium using the Quantikine® Human IGF Immunoassay ELISA kit (R &D Systems). HRECs were treated with either 5.5 or 25 mM glucose and aliquots were taken daily for analysis.

Isolation of protein from HRECs: Cells were grown in 150 mm tissue culture plates and transfected as described above. The cells were washed with ice cold phosphate buffered saline (PBS; catalog number MT21-040-CV, Mediatech, Herndon, VA) and scraped in 30 ml of lysis buffer (150 mM Tris-HCL, 150 mM NaCl, 1 mM EDTA, 1% Igepal CA-630 (Sigma, St. Louis, MO) 1% protease inhibitor cocktail (Sigma), 1 mM DTT [Fisher Scientific, Pittsburgh, PA]). The lysed cells were sonicated for 20 s and centrifuged at 16,100x g for 15 min at 4 °C. The pellet was discarded and the amount of protein in the supernatant was determined using a bicinchoninic acid (BCA) protein assay kit (Pierce, Rockford, IL).

FACS analysis: Transfected cells were harvested 48 h following transfection. Cells were lifted off the plate using a cell stripper (Mediatech) and centrifuged to pellet the cells. The cell pellets were suspended in 1 ml of 0.1% BSA in 10 mM NaCl and kept on ice for the remainder of the procedure. An equal amount (10 μg) of either VEGFR-1 antibody (Santa Cruz Biotechnology Inc., Santa Cruz, CA) or VEGFR-2 antibody (Neomarkers, Fremont, CA) was added to the cells and the cells incubated for 30 min on ice. The cells were then washed twice with 0.1% BSA and incubated with 22.5 μg of goat anti-rabbit-FITC antibody (Jackson Immuno Research, West Grove, PA) in 1 ml of 0.1% BSA for 30 min in the dark. The cells were washed twice with 0.1% BSA and 5000 cells analyzed on a FACScan (BD Biosciences, San Jose, CA).

The effect of glucose on the phosphorylation of VEGFR-1 and VEGFR-2: Confluent cultures were exposed to microvascular endothelial cell basal medium containing either 5.5 or 25 mM D-glucose for up to 6 h. Cells were lysed in RIPA buffer (50 mM Tris-HCL, pH 7.4, 150 mM NaCl, 1% NP-40, 0.25% sodium deoxycholate, 1 mM NaF, 1 mM Na_3VO_4, and 1 mM EDTA containing protease inhibitors phenylmethylsulfonyl fluoride, aprotonin, leupeptin, and pepstatin) at 4 °C for 30 min. The lysate was centrifuged at 12,000x g for 20 min, and the protein content of the supernatant was determined using the Coomassie blue technique (BioRad). To determine the phosphorylation status of VEGFR-1 and VEGFR-2, phosphorylated proteins were immunoprecipitated from the microvascular endothelial cell lysate (suspended in PBS (Mediatech) at a final concentration of 200 μg cell pellet/ml PBS) by 10 μl mouse anti-tyrosine phosphorylation monoclonal antibody (PY 20; BD Biosciences, San Jose, CA) for 1.5 h at 4 °C followed by addition of 20 μl protein A/G agarose (Santa Cruz Biotechnology) overnight at 4 °C. After the mixture was washed with RIPA buffer, it was centrifuged at 12,000x g for 20 min. The pellet was mixed with 40

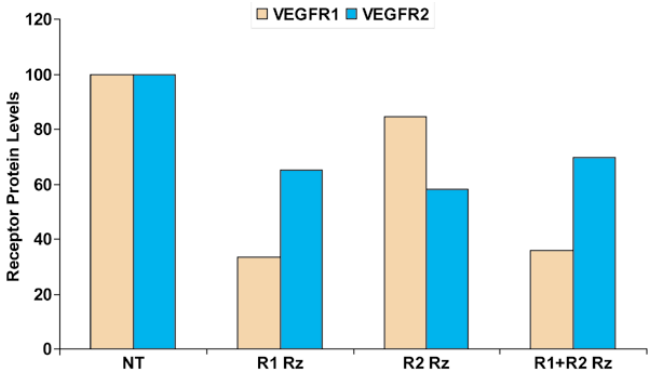

Figure 3. Reduction of vascular endothelial growth factor (VEGF) receptor levels following transfection with ribozymes. Transfection with the VEGFR-1 ribozyme reduced VEGFR-1 surface expression while also reducing VEGFR-2 levels. Transfection with VEGFR-2 ribozyme reduced VEGFR-2 levels and also VEGFR-1 levels. These results suggest a level of coregulation of VEGF receptor expression. The graph shows non-transfected HRECs (NT), HRECs transfected with the VEGFR-1 ribozyme (R1 Rz), and HRECs transfected with the VEGFR-2 ribozyme (R2 Rz), and HRECs tranfected with both the VEGFR-1 and VEGFR-2 ribozymes (R1+R2 Rz).

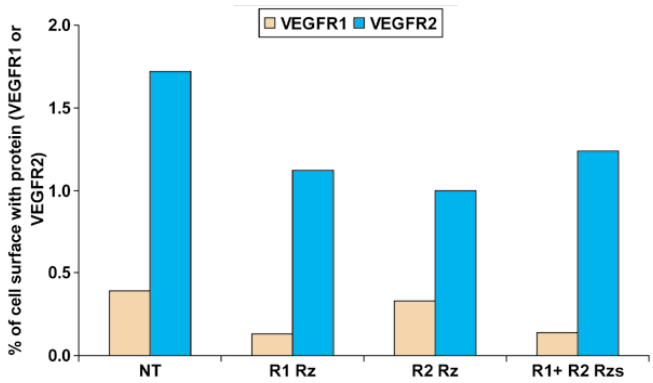

Figure 4. Percent of the human retinal endothelial cell (HREC) surface expressing the VEGF receptor. HRECs express lower levels of VEGFR-1 than VEGFR-2 basally. Reduction of VEGFR-1 results in a coordinate reduction of VEGFR-2, whereas reduction of VEGFR-2 has less of an impact on VEGFR-1 expression. The graph shows non-transfected HRECs (NT), HRECs transfected with the VEGFR-1 ribozyme (R1 Rz), and HRECs transfected with the VEGFR-2 ribozyme (R2 Rz), and HRECs tranfected with both the VEGFR-1 and VEGFR-2 ribozymes (R1+R2 Rz).

µl 1X Laemmli buffer, heated at 80 °C for 5 min and subjected to SDS-PAGE and western blotting using antibodies against VEGFR-1 and VEGFR-2 (Santa Cruz Biotechnology).

Western analysis for occludin: A total of 80 µg of protein was separated on a Criterion 4-15% gradient polyacrylamide gel (BioRad) at 120 V for 20 min and 140 V for 65 min and transferred (80 V for 5 h) to a nitrocellulose membrane (Millipore Corp., Bedford, MA) using a blot cell apparatus (BioRad) on ice at 4 °C. The membranes were blocked in TBS containing 0.05% Tween-20 (Sigma) and 5% milk for 1 h at room temperature. For occludin detection, the membrane was incubated with anti-rabbit occludin antibody (2 µg/ml; Zymed Laboratories Inc., San Francisco, CA) at 4 °C overnight. Blots were then washed with TBS containing 0.05% Tween and 5% milk 5% (w/v) nonfat dry milk for 5 min and incubated with a 1:2000 dilution of horseradish peroxidase (HRP)-conjugated mouse ant-rabbit antibody (Santa Cruz Biotechnology) for 1 h at room temperature. After being incubated with the secondary antibody, the membranes were washed twice for 5 min and twice for 10 min with (TBS containing 0.05% Tween-20).

After occludin protein detection, the membranes were also used to detect β-actin protein levels. The levels of β-actin were determined with the same protocol used to determine occludin levels. The primary antibody was mouse monoclonal anti-β-actin antibody (1:5000 dilution, Sigma) and the secondary antibody HRP-conjugated anti-mouse IgG (1:7500 dilution, Sigma). The protein bands were visualized on X-ray film with an enhanced chemiluminescence (ECL) western blot detection kit (GE Healthcare, Fairfield, CT). Standard molecular weight markers (BioRad) served to verify the molecular size of occludin at 65 kDa and of β-actin at 42 kDa. Analysis of occludin and β-actin protein levels were performed on scanned X-ray film images using ScionImage (version 4.0.3.2; Scion Corp., Frederick, MD).

Occludin immunolocalization by immunostaining: To study the distribution pattern and relative amounts of occludin immunofluorescence staining was performed on HRECs grown to confluence in low (5.5 mM) and high (25 mM) glucose on 2% gelatin and fibronectin (5 µg/ml)-coated chamber slides (Lab-Tek, Naperville, IL). HRECs were washed with PBS and fixed with freshly prepared 4% paraformaldehyde for 15 min, permeabilized with 0.1% Triton X-100 for 5 min, and then blocked with PBS containing 10% normal goat serum for 30 min at room temperature. After washing in PBS containing 100 mM glycine, primary antibody to rabbit anti-occludin (20 µg/ml; Zymed) in blocking buffer was added and cells incubated for 1 h on ice. After three PBS washes, the secondary antibody, fluorescein isothiocyanate-conjugated goat anti-rabbit IgG (1:200 dilution, Vector Labs., Burlingame,

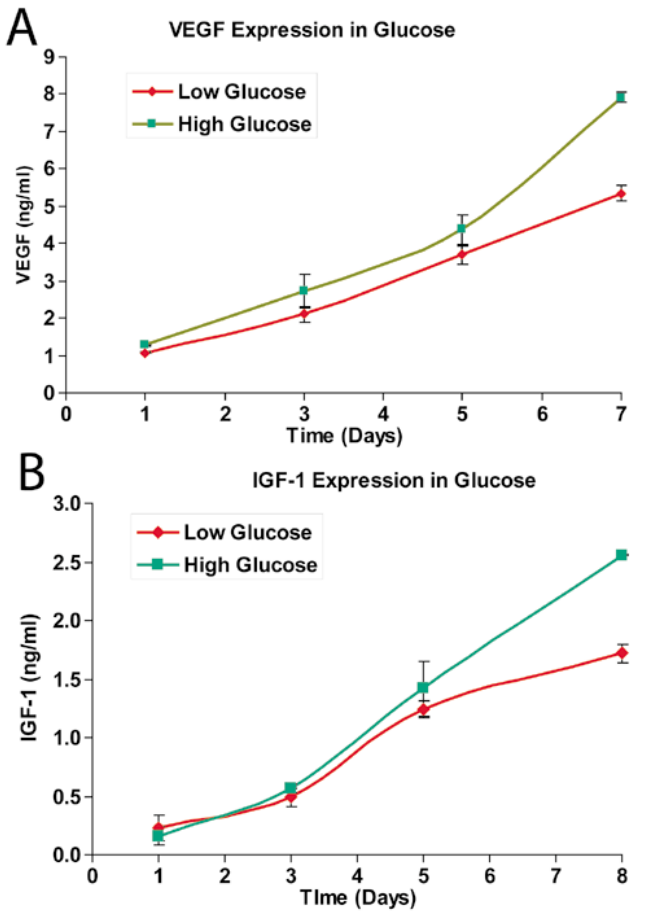

Figure 5. Effect of high glucose on growth factor expression in human retinal endothelial cells (HRECs). Exposure of HRECs to high glucose conditions resulted in a time-dependent increase in both vascular endothelial growth factor (VEGF) and insulin-like growth factor I (IGF-I) levels. Effect of high glucose on growth factor expression in human retinal endothelial cells (HRECs). Exposure of HRECs to high glucose conditions (green lines) resulted in a time-dependent increase in both VEGF (**A**) and IGF-I (**B**) levels greater than seen in low glucose conditions (red lines).

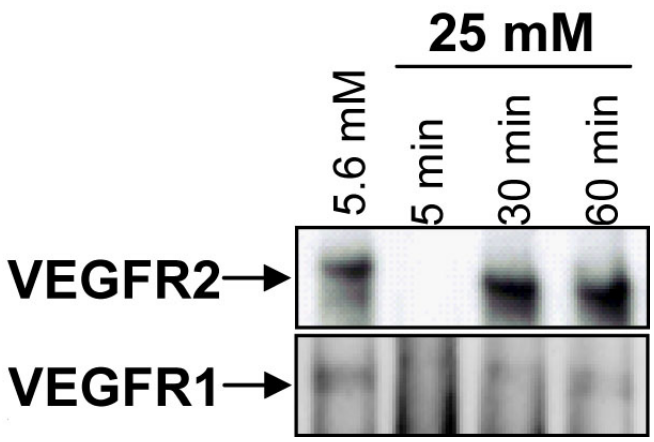

Figure 6. Effect of glucose on VEGFR-1 and VEGFR-2 phosphorylation in HRECs. Lysates from HRECs grown under low glucose (5.5 mM) or high glucose (25 mM) conditions were immunoprecipitated to isolate the phosphorylated versions of VEGFR-1 and VEGFR-2. Immunoprecipitated proteins were then analyzed by western blotting and detected with antibodies to VEGFR-1 or VEGFR-2. Exposure to 25 mM glucose resulted in an increase in VEGFR-2 phosphorylation at 30 min and 1 h in HRECs. Exposure to 25 mM glucose had minimal effect on VEGFR-1 phosphorylation.

CA), was applied to the cells for 30 min at room temperature. After three PBS washes the cells were covered with Vecta-Shield DAPI (Vector Labs) for nuclear staining and a coverslip. Negative control samples were processed in exactly the same way except that the primary antibody was omitted. The cells were viewed and photographed using a fluorescence microscope (Axiovert 135; Carl Zeiss, Thornwood, NY).

Statistical analysis: Data was analyzed using the Student's t-test and reported as mean±standard deviation (SD). A p value <0.05 was considered significant.

RESULTS

Hammerhead ribozymes reduce expression of VEGFR-1, VEGFR-2, and IGF-IR mRNAs: We designed and tested three hammerhead ribozymes that are specific for mRNAs of VEGFR-1, VEGFR-2, and IGF-IR. All ribozymes were cloned into expression vectors for transfection of HRECs [38]. Figure 1 shows the time course of cleavage analysis for all three ribozymes on 13-nucleotide RNA target oligonucleotides and demonstrates that the catalytic activities of VEGFR-1, VEGFR-2, and IGF-IR are similar. This figure also demonstrates that the VEGFR-1 and VEGFR-2 ribozymes will only cleave their respective targets.

Plasmids expressing the VEGFR-1 and VEGFR-2 ribozymes and the expression plasmid p21NewHp [39] were transfected into HRECs to determine their effect on expression of VEGFR-1 and VEGFR-2 mRNAs. Reverse transcription was performed on total RNA isolated from HRECs. Figure 2 shows the results of real time PCR performed on reverse transcription products used to determine the levels of VEGFR-1 and VEGFR-2 mRNA relative to β-actin. Transfection with the active VEGFR-1 ribozyme resulted in a reduction of the VEGFR-1 mRNA by 71.1±2.1%, ($p<0.0002$). Transfection with the active VEGFR-2 resulted in a reduction of VEGFR-2 mRNA levels by 85.1±1.9%, ($p<0.008$). Similarly, previous transfection with the active IGF-IR ribozyme resulted in a reduction of IGF-IR mRNA levels by 70.5±10.1%, ($p<0.003$) [39].

FACS analysis was performed to confirm reduction of expression of the respective receptors as shown in Figure 3. The transfection of HRECs with the ribozyme to VEGFR-1 resulted in a reduction of VEGFR-1 surfaces expression by 67%; however, VEGFR-2 levels were also reduced by 35% of original levels with the VEGFR-1 ribozyme. Transfection with the VEGFR-2 ribozyme resulted in reduction of VEGFR-2 by 42% of original levels and VEGFR-1 by 15% of the original

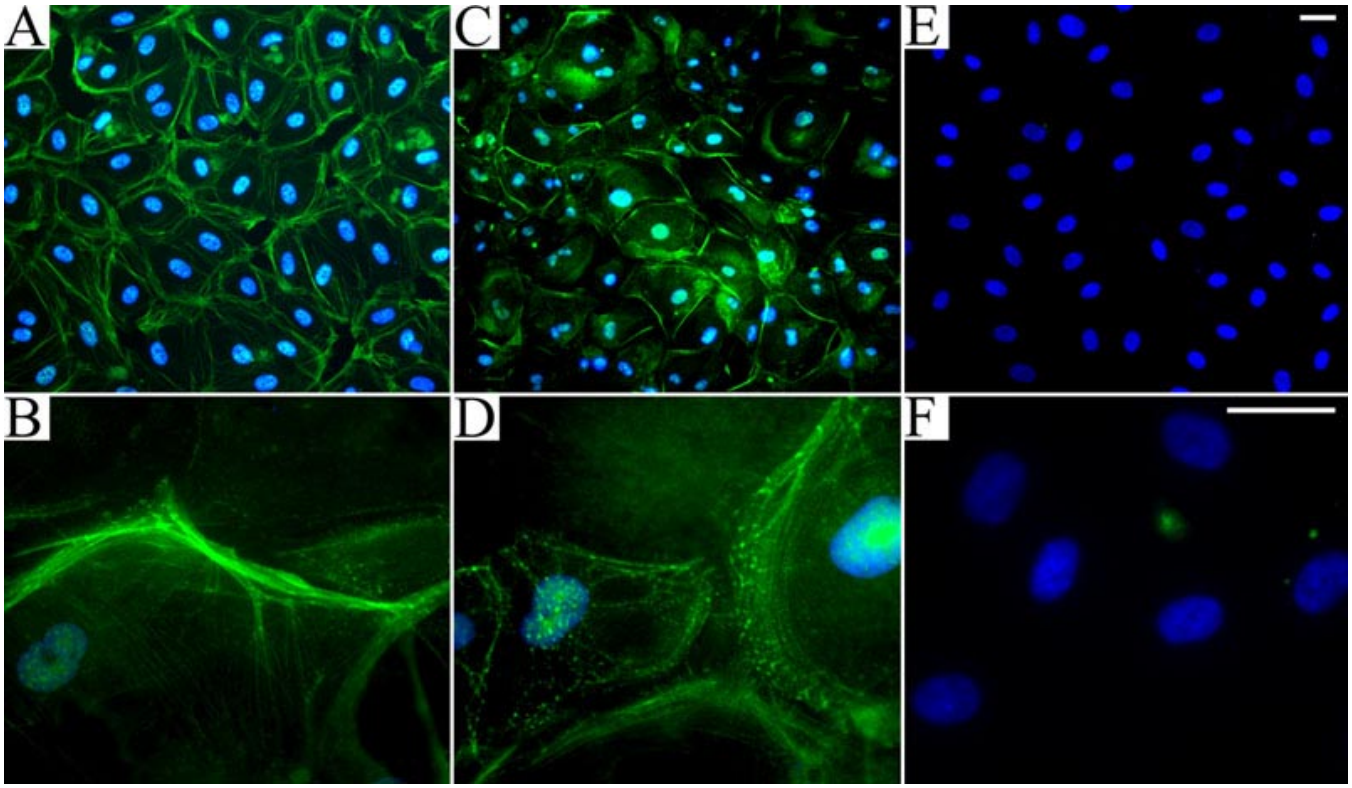

Figure 7. Loss of tight junction integrity in human retinal endothelial cells (HRECs) grown in 25 mM glucose. Representative photomicrographs of HRECs grown in low glucose medium (**A**,**B**,**E**,**F**) or high glucose medium (**C**,**D**). **A**-**D**: Tight junctions are visualized with an antibody to occludin (FITC, green) and nuclei are visualized with DAPI (blue). **E**,**F**: Controls for background were not treated with the occludin antibody; nuclei are visualized with DAPI (blue). Note the reduced fluorescence and disruption of the tight junctions formed between HRECs grown in high glucose (**C**,**D**) compared to HRECs grown in low glucose (**A**,**B**). Less occludin detection with clear areas of disruption are seen (**C**); however, some cytoplasmic autofluorescence is evident. The original magnifications were 200x (**A**,**C**,**E**) and 630x (**B**,**D**,**F**). The scale bars represent 50 μm.

levels. Cotransfection of both ribozymes resulted in reduction of VEGFR-1 levels by 64% of initial levels and reduction of VEGFR-2 by 30% of the initial levels. While the ribozymes were highly specific for their own targets and did not cleave mRNA for the other receptor, they appeared to reduce levels of the other receptor. These results suggest a level of coregulation of expression between these two receptors. Analysis of the percent of the cell surface expressing the respective receptor protein demonstrated that HREC express lower levels of VEGFR-1 than VEGFR-2 basally and that reduction of VEGFR-1 results in a coordinate reduction of VEGFR-2, whereas reduction of VEGFR-2 has less of an impact on VEGFR-1 expression (Figure 4).

Effect of high glucose on growth factor expression in HRECs: Exposure of HRECs to high glucose conditions resulted in a significant increase in both VEGF and IGF-I levels by day 8 (Figure 5).

Effect of glucose on VEGFR-1 and VEGFR-2 phosphorylation: Cells exposed to 5.5 mM glucose demonstrated significant phosphorylation of VEGFR-2 and weak phosphorylation of VEGFR-1 (Figure 6). Exposure to 25 mM glucose resulted in an initial decrease in VEGFR-2 phosphorylation followed by a large increase in VEGFR-2 phosphorylation at 30 min and 1 h.

Effect of high glucose on occludin expression: The distribution of occludin expression was determined using immunofluorescence microscopy. Under normal glucose conditions the fluorescent staining for occludin was located to the lateral membranes of the endothelial cells (Figure 7A,B). By contrast high glucose conditions resulted in a decrease in occludin staining, which became more diffusely distributed on the lateral membranes with evidence of focal aggregation between adjacent cells (Figure 7C,D). Nonspecific staining of the cytoplasm was apparent, however, in some cells (Figure 7C,D,F).

Reduction in expression of VEGFR-1, VEGFR-2, and IGF-IR prevents occludin downregulation in high glucose: We isolated protein from HRECs transfected with plasmids expressing the VEGFR-1, VEGFR-2, and IGFR-1R ribozymes, and we used western analysis to examine occludin levels (Figure 8) in the isolated protein. Occludin levels in nontransfected HRECs grown in high glucose were significantly reduced by (19%±1.75%, $p<0.0002$) compared to HRECs grown in low glucose. Similarly, occludin levels in HRECs grown in high glucose and transfected with control vector (p21NewHp) were reduced by (38%±4.1%, $p<0.0002$) compared to HRECs grown in normal glucose.

HRECs grown in high glucose and transfected with active VEGFR-1, VEGFR-2, or IGF-IR ribozymes did not have reduced occludin levels. The combination of the VEGFR-1 and VEGFR-2 ribozymes increased occludin levels in high glucose by (54%±16%, $p=0.02$) over low glucose levels.

DISCUSSION

The major findings of this report are that the tight junction protein, occludin, decreases in HRECs grown in high glucose. Furthermore, hammerhead ribozymes against VEGFR-1, VEGFR-2, or IGF-IR prevented this downregulation of occludin. That both VEGFR-1 and VEGFR-2 ribozymes prevented the glucose-induced downregulation of occludin suggests the involvement of both VEGF receptors in glucose-induced permeability. The effect of VEGF on vascular permeability is well established, yet the mechanisms of this action remains poorly understood. VEGFR-2 has been implicated in VEGF-induced permeability [17] although receptor cross-talk may also play a role [19]. In support of this, we have shown that transfection of HRECs with VEGFR-1 ribozyme down regulated the VEGFR-2 mRNA. This may explain in part the beneficial effect observed with the VEGFR-1 ribozyme. The transfection of HRECs with VEGFR-2 ribozyme down regulated VEGFR-2 and also VEGFR-1 mRNAs. This has been previously observed and supports intra- and intermolecular cross-talk between VEGF receptors [45]. Numerous studies have shown that VEGFR-1 can negatively regulate VEGFR-2 action through different intramolecular mechanisms including the PI3 kinase pathway and nitric oxide [45-47]. Our study suggests that the opposite also may be true and that VEGFR-2 regulates VEGFR-1.

It is clear from our study that high glucose was able to

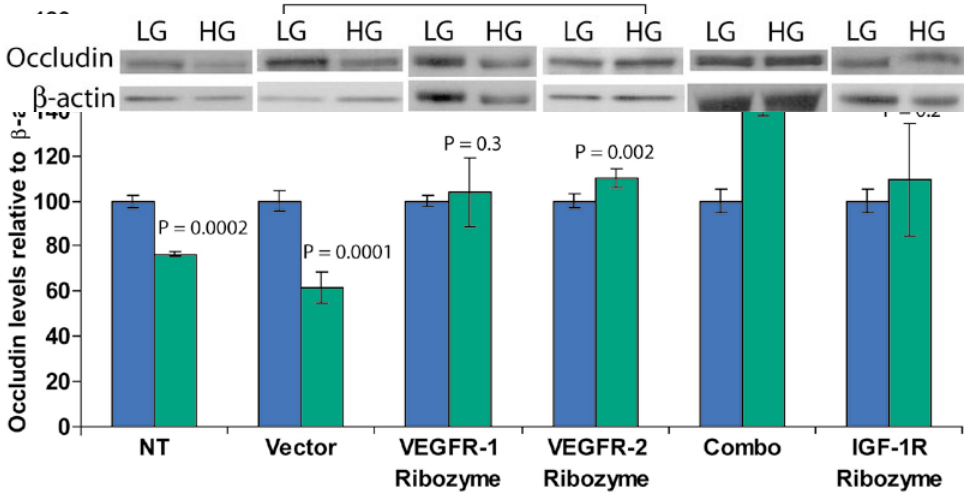

Figure 8. Occludin downregulatin in low glucose is prevented by ribozyme expression. Western analysis demonstrates that the VEGFR-1, VEGFR-2, and IGF-IR ribozymes prevent occludin downregulation in high glucose. The blue bars represent occludin levels in HRECs grown in low glucose (set to 100%) and the green bars represent HRECs grown in high glucose. "Combo" represents occludin levels isolated from HRECs transfected with both the VEGFR-1 and VEGFR-2 ribozymes. Occludin levels were determined relative to β-actin.

activate VEGFR-2 but not VEGFR-1. The phosphorylation of VEGFR-2 in high glucose is not unexpected since high glucose is known to stimulate VEGF expression [48]. However, this may be temporally regulated since dephosphorylation was observed following 5 min exposure to high glucose prior to a significant increase in VEGFR-2 phosphorylation at 30 and 60 min. The VEGFR-1 response is not unexpected since VEGFR-1 is typically weakly phosphorylated in response to ligand binding.

Our study suggests that both VEGF and IGF-I family members can regulate vascular permeability through occludin expression. However, the ability of VEGF to increase permeability may arise from a number of other mechanisms distinct from its effects on occludin. VEGF may stimulate endocytosis and vesicular transport by inducing fenestrations and fused clustered caveolae-like vesicles known as vesiculovacuolar organelles (VVOs) [49], which have been observed in endothelial cells in vitro [50]. VVOs occur consistently in tumor vessels known to be leaky [51]. However, in vivo studies have shown that the vasculature of the retina does not contain many vesicles [52] and production of VVOs in retinal blood vessels has not been reported in diabetes. Others propose that permeability may also include paracellular routes in which solutes diffuse between cells [53]. VEGF-induced permeability has also been shown to be mediated by activation of urokinase plasminogen activator (uPA) and its receptor (uPAR) causing downregulation of occludin [54]. uPA cleaves tissue plasminogen into the active enzyme plasmin, which in turn has been shown to activate latent TGF-β1 [55] that subsequently induces increased permeability via VEGFR-1 and VEGFR-2. VEGF-induced permeability also involves interaction with a variety of other factors and pathways. Nitric oxide (NO) generation and subsequent activation of extracellular signal-regulated kinase (ERK), mitogen-activated kinase (MAK) [56], prostacyclin generation [17], or VEGF-induced protein kinase C (PKC) activity [57] have all been proposed to contribute to increased vascular permeability. NO disrupts both cytoskeletal protein complexing in cells and the arrangement of the actin cytoskeleton [11,58-60], resulting in dilation of the tight junction due to ATP depletion [60]. Recent studies, using streptozotocin-induced diabetic rats have shown that the initial BRB breakdown is associated with increases in expression of both neuronal and endothelial NO synthetase (nNOS and eNOS, respectively) as well as increases in VEGF expression [10,61,62]. Moreover, a VEGF neutralizing receptor construct has been shown to prevent diabetes-induced increases in expression of VEGF and eNOS, and prevent breakdown of the BRB [12,62].

The reason for the disappearance and reorganization of occludin protein may be linked with phosphorylation since activation of VEGF signaling pathways results in the phosphorylation of tight junction proteins occludin and ZO-1 [11], creating leaky endothelial cell-cell contacts [63,64]. Recently, it has been shown that tyrosine phosphorylation of the C-terminal tail of occludin resulted in a reduced interaction with ZO-1, ZO-2, and ZO-3 that may prevent the assembly of the tight junction or destabilize it. In addition, the C-terminal tail of occludin binds c-Src, suggesting a possible role of the Src family kinases in the regulation of the tight junction [65].

Autocrine regulation of HRECs is supported by the observation that HRECs express protein and mRNA for IGF-IR, VEGFR-1, and VEGFR-2 [39,66], and the HRECs secrete their ligands, VEGF and IGF-I. Furthermore, VEGF and IGF-I may interact since elevated IGF-I levels in vivo increase VEGF gene expression [32] and may contribute to the vascular permeability changes observed in diabetes. This is supported by (1) our previous observations that intravitreal injections of IGF-I result in an acute increase in vascular permeability and vascular engorgement, followed by development of preretinal angiogenesis in rabbit eyes [67]; and (2) IGF-I production by HRECs in turn stimulates increased VEGF production [33] and vice versa [68]. This IGF-I/VEGF interaction could account for the reduction of occludin protein observed.

Our findings indicate that hammerhead ribozymes targeted for VEGFR-1, VEGFR-2, and IGF-IR are potentially useful in regulating vascular permeability. Hammerhead ribozymes, the catalytic RNA molecules that cleave phosphodiester bonds between RNA nucleotides [36], offer the potential to block expression of genes prior to protein translation. Because of their catalytic activity, a lower concentration of ribozyme molecules is required to achieve inhibition of mRNA expression compared to antisense oligonucleotides. However, the application of these ribozymes to prevent vascular permeability in conditions, such as diabetic macular edema, requires in vivo delivery. We have demonstrated the in vivo efficacy of the IGF-IR ribozyme in inhibiting preretinal neovascularization in the oxygen-induced retinopathy model [39]. VEGFR-1 and VEGFR-2 hammerhead ribozymes demonstrate similar inhibition [69].

In conclusion, our results demonstrate that high glucose induces expression of VEGF and IGF-I in HRECs, and glucose directly or indirectly induces phosphorylation of VEGFR-2 but not VEGFR-1. The expression of VEGFR-1 and VEGFR-2 appear to be coregulated as they influence the levels of each other's mRNA. All three receptors are involved in regulating occludin levels as VEGFR-1, VEGFR-2, and IGF-IR ribozymes reverse the effect of high glucose-induced changes in occludin content in HRECs. The end result is that the reduced expression of occludin by RECs leads to structural failure and BRB breakdown. Thus, it is conceivable that delivery of VEGFR-1, VEGFR-2 and IGF-IR ribozymes in retinal vascular cells could provide a powerful means of regulating BRB permeability and a tool in the understanding of the pathophysiogy of diabetic retinopathy.

ACKNOWLEDGEMENTS

This project was funded by grants from the NIH (R01EY07739 and R01EY12601) and the Juvenile Diabetes Research Foundation.

REFERENCES

1. Cunha-Vaz J, Faria de Abreu JR, Campos AJ. Early breakdown of the blood-retinal barrier in diabetes. Br J Ophthalmol 1975; 59:649-56.

2. Enea NA, Hollis TM, Kern JA, Gardner TW. Histamine H1 receptors mediate increased blood-retinal barrier permeability in experimental diabetes. Arch Ophthalmol 1989; 107:270-4.
3. Do carmo A, Ramos P, Reis A, Proenca R, Cunha-vaz JG. Breakdown of the inner and outer blood retinal barrier in streptozotocin-induced diabetes. Exp Eye Res 1998; 67:569-75.
4. Gardner TW, Antonetti DA, Barber AJ, LaNoue KF, Levison SW. Diabetic retinopathy: more than meets the eye. Surv Ophthalmol 2002; 47:S253-62.
5. Furuse M, Hirase T, Itoh M, Nagafuchi A, Yonemura S, Tsukita S, Tsukita S. Occludin: a novel integral membrane protein localizing at tight junctions. J Cell Biol 1993; 123:1777-88.
6. McCarthy KM, Skare IB, Stankewich MC, Furuse M, Tsukita S, Rogers RA, Lynch RD, Schneeberger EE. Occludin is a functional component of the tight junction. J Cell Sci 1996; 109:2287-98.
7. Barber AJ, Lieth E, Khin SA, Antonetti DA, Buchanan AG, Gardner TW. Neural apoptosis in the retina during experimental and human diabetes. Early onset and effect of insulin. J Clin Invest 1998; 102:783-91.
8. Antonetti DA, Barber AJ, Khin S, Lieth E, Tarbell JM, Gardner TW. Vascular permeability in experimental diabetes is associated with reduced endothelial occludin content: vascular endothelial growth factor decreases occludin in retinal endothelial cells. Penn State Retina Research Group. Diabetes 1998; 47:1953-9.
9. Barber AJ, Antonetti DA. Mapping the blood vessels with paracellular permeability in the retinas of diabetic rats. Invest Ophthalmol Vis Sci 2003; 44:5410-6.
10. Aiello LP, Avery RL, Arrigg PG, Keyt BA, Jampel HD, Shah ST, Pasquale LR, Thieme H, Iwamoto MA, Park JE, Nguyen HV, Aiello LM, Ferrara N, King GL. Vascular endothelial growth factor in ocular fluid of patients with diabetic retinopathy and other retinal disorders. N Engl J Med 1994; 331:1480-7.
11. Antonetti DA, Barber AJ, Hollinger LA, Wolpert EB, Gardner TW. Vascular endothelial growth factor induces rapid phosphorylation of tight junction proteins occludin and zonula occluden 1. A potential mechanism for vascular permeability in diabetic retinopathy and tumors. J Biol Chem 1999; 274:23463-7.
12. Qaum T, Xu Q, Joussen AM, Clemens MW, Qin W, Miyamoto K, Hassessian H, Wiegand SJ, Rudge J, Yancopoulos GD, Adamis AP. VEGF-initiated blood-retinal barrier breakdown in early diabetes. Invest Ophthalmol Vis Sci 2001; 42:2408-13.
13. Terman BI, Dougher-Vermazen M, Carrion ME, Dimitrov D, Armellino DC, Gospodarowicz D, Bohlen P. Identification of the KDR tyrosine kinase as a receptor for vascular endothelial cell growth factor. Biochem Biophys Res Commun 1992; 187:1579-86.
14. Millauer B, Wizigmann-Voos S, Schnurch H, Martinez R, Moller NP, Risau W, Ullrich A. High affinity VEGF binding and developmental expression suggest Flk-1 as a major regulator of vasculogenesis and angiogenesis. Cell 1993; 72:835-46.
15. Fong Y, Federoff HJ, Brownlee M, Blumberg D, Blumgart LH, Brennan MF. Rapid and efficient gene transfer in Human hepatocytes by herpes viral vectors. Hepatology 1995; 22:723-9.
16. Cai J, Boulton M. The pathogenesis of diabetic retinopathy: old concepts and new questions. Eye 2002; 16:242-60.
17. Murohara T, Horowitz JR, Silver M, Tsurumi Y, Chen D, Sullivan A, Isner JM. Vascular endothelial growth factor/vascular permeability factor enhances vascular permeability via nitric oxide and prostacyclin. Circulation 1998; 97:99-107.
18. Soker S, Takashima S, Miao HQ, Neufeld G, Klagsbrun M. Neuropilin-1 is expressed by endothelial and tumor cells as an isoform-specific receptor for vascular endothelial growth factor. Cell 1998; 92:735-45.
19. Stacker SA, Vitali A, Caesar C, Domagala T, Groenen LC, Nice E, Achen MG, Wilks AF. A mutant form of vascular endothelial growth factor (VEGF) that lacks VEGF receptor-2 activation retains the ability to induce vascular permeability. J Biol Chem 1999; 274:34884-92.
20. Ideta R, Yamashita H, Tanaka Y, Kato S, Kitano S, Hori S. Roles of cytokines in diabetic retinopathy. Arch Ophthalmol 1999; 117:700-1.
21. Merimee TJ, Zapf J, Froesch ER. Insulin-like growth factors. Studies in diabetics with and without retinopathy. N Engl J Med 1983; 309:527-30.
22. Dills DG, Moss SE, Klein R, Klein BE. Association of elevated IGF-I levels with increased retinopathy in late-onset diabetes. Diabetes 1991; 40:1725-30.
23. Henricsson M, Berntorp K, Berntorp E, Fernlund P, Sundkvist G. Progression of retinopathy after improved metabolic control in type 2 diabetic patients. Relation to IGF-1 and hemostatic variables. Diabetes Care 1999; 22:1944-9.
24. Hyer SL, Sharp PS, Brooks RA, Burrin JM, Kohner EM. A two-year follow-up study of serum insulinlike growth factor-I in diabetics with retinopathy. Metabolism 1989; 38:586-9.
25. Chantelau E, Eggert H, Seppel T, Schonau E, Althaus C. Elevation of serum IGF-1 precedes proliferative diabetic retinopathy in Mauriac's syndrome. Br J Ophthalmol 1997; 81:169-70.
26. Brausewetter F, Jehle PM, Jung MF, Boehm BO, Brueckel J, Hombach V, Osterhues HH. Microvascular permeability is increased in both types of diabetes and correlates differentially with serum levels of insulin-like growth factor I (IGF-I) and vascular endothelial growth factor (VEGF). Horm Metab Res 2001; 33:713-20.
27. Grant M, Russell B, Fitzgerald C, Merimee TJ. Insulin-like growth factors in vitreous. Studies in control and diabetic subjects with neovascularization. Diabetes 1986; 35:416-20.
28. Meyer-Schwickerath R, Pfeiffer A, Blum WF, Freyberger H, Klein M, Losche C, Rollmann R, Schatz H. Vitreous levels of the insulin-like growth factors I and II, and the insulin-like growth factor binding proteins 2 and 3, increase in neovascular eye disease. Studies in nondiabetic and diabetic subjects. J Clin Invest 1993; 92:2620-5.
29. Boulton M, Gregor Z, McLeod D, Charteris D, Jarvis-Evans J, Moriarty P, Khaliq A, Foreman D, Allamby D, Bardsley B. Intravitreal growth factors in proliferative diabetic retinopathy: correlation with neovascular activity and glycaemic management. Br J Ophthalmol 1997; 81:228-33.
30. Danis RP, Bingaman DP. Insulin-like growth factor-1 retinal microangiopathy in the pig eye. Ophthalmology 1997; 104:1661-9.
31. Grant MB, Mames RN, Fitzgerald C, Ellis EA, Aboufriekha M, Guy J. Insulin-like growth factor I acts as an angiogenic agent in rabbit cornea and retina: comparative studies with basic fibroblast growth factor. Diabetologia 1993; 36:282-91.
32. Punglia RS, Lu M, Hsu J, Kuroki M, Tolentino MJ, Keough K, Levy AP, Levy NS, Goldberg MA, D'Amato RJ, Adamis AP. Regulation of vascular endothelial growth factor expression by insulin-like growth factor I. Diabetes 1997; 46:1619-26.
33. Smith LE, Shen W, Perruzzi C, Soker S, Kinose F, Xu X, Robinson G, Driver S, Bischoff J, Zhang B, Schaeffer JM, Senger DR. Regulation of vascular endothelial growth factor-dependent retinal neovascularization by insulin-like growth factor-1 receptor. Nat Med 1999; 5:1390-5.
34. Grant MB, Tarnuzzer RW, Caballero S, Ozeck MJ, Davis MI,

Spoerri PE, Feoktistov I, Biaggioni I, Shryock JC, Belardinelli L. Adenosine receptor activation induces vascular endothelial growth factor in human retinal endothelial cells. Circ Res 1999; 85:699-706.
35. Fritz JJ, Lewin A, Hauswirth W, Agarwal A, Grant M, Shaw L. Development of hammerhead ribozymes to modulate endogenous gene expression for functional studies. Methods 2002; 28:276-85.
36. Cech TR. RNA as an enzyme. Biochem Int 1989; 18:7-14.
37. Shimayama T. Effects of deoxyribonucleotide substitutions in the substrate strand on hammerhead ribozyme-catalyzed reactions. Gene 1994; 149:41-6.
38. Shaw LC, Skold A, Wong F, Petters R, Hauswirth WW, Lewin AS. An allele-specific hammerhead ribozyme gene therapy for a porcine model of autosomal dominant retinitis pigmentosa. Mol Vis 2001; 7:6-13.
39. Shaw LC, Afzal A, Lewin AS, Timmers AM, Spoerri PE, Grant MB. Decreased expression of the insulin-like growth factor 1 receptor by ribozyme cleavage. Invest Ophthalmol Vis Sci 2003; 44:4105-13.
40. Afzal A, Shaw LC, Caballero S, Spoerri PE, Lewin AS, Zeng D, Belardinelli L, Grant MB. Reduction in preretinal neovascularization by ribozymes that cleave the A2B adenosine receptor mRNA. Circ Res 2003; 93:500-6.
41. Grant MB, Guay C. Plasminogen activator production by human retinal endothelial cells of nondiabetic and diabetic origin. Invest Ophthalmol Vis Sci 1991; 32:53-64.
42. Grant MB, Davis MI, Caballero S, Feoktistov I, Biaggioni I, Belardinelli L. Proliferation, migration, and ERK activation in human retinal endothelial cells through A(2B) adenosine receptor stimulation. Invest Ophthalmol Vis Sci 2001; 42:2068-73.
43. Wong HC, Boulton M, Marshall J, Clark P. Growth of retinal capillary endothelia using pericyte conditioned medium. Invest Ophthalmol Vis Sci 1987; 28:1767-75.
44. Ohki EC, Tilkins ML, Ciccarone VC, Price PJ. Improving the transfection efficiency of post-mitotic neurons. J Neurosci Methods 2001; 112:95-9.
45. Autiero M, Waltenberger J, Communi D, Kranz A, Moons L, Lambrechts D, Kroll J, Plaisance S, De Mol M, Bono F, Kliche S, Fellbrich G, Ballmer-Hofer K, Maglione D, Mayr-Beyrle U, Dewerchin M, Dombrowski S, Stanimirovic D, Van Hummelen P, Dehio C, Hicklin DJ, Persico G, Herbert JM, Communi D, Shibuya M, Collen D, Conway EM, Carmeliet P. Role of PlGF in the intra- and intermolecular cross talk between the VEGF receptors Flt1 and Flk1. Nat Med 2003; 9:936-43.
46. Bussolati B, Dunk C, Grohman M, Kontos CD, Mason J, Ahmed A. Vascular endothelial growth factor receptor-1 modulates vascular endothelial growth factor-mediated angiogenesis via nitric oxide. Am J Pathol 2001; 159:993-1008.
47. Zeng H, Dvorak HF, Mukhopadhyay D. Vascular permeability factor (VPF)/vascular endothelial growth factor (VEGF) peceptor-1 down-modulates VPF/VEGF receptor-2-mediated endothelial cell proliferation, but not migration, through phosphatidylinositol 3-kinase-dependent pathways. J Biol Chem 2001; 276:26969-79.
48. Zhao B, Cai J, Boulton M. Expression of placenta growth factor is regulated by both VEGF and hyperglycaemia via VEGFR-2. Microvasc Res 2004; 68:239-46.
49. Roberts WG, Palade GE. Increased microvascular permeability and endothelial fenestration induced by vascular endothelial growth factor. J Cell Sci 1995; 108:2369-79.
50. Esser S, Wolburg K, Wolburg H, Breier G, Kurzchalia T, Risau W. Vascular endothelial growth factor induces endothelial fenestrations in vitro. J Cell Biol 1998; 140:947-59.
51. Qu-Hong, Nagy JA, Senger DR, Dvorak HF, Dvorak AM. Ultrastructural localization of vascular permeability factor/vascular endothelial growth factor (VPF/VEGF) to the abluminal plasma membrane and vesiculovacuolar organelles of tumor microvascular endothelium. J Histochem Cytochem 1995; 43:381-9.
52. Sagaties MJ, Raviola G, Schaeffer S, Miller C. The structural basis of the inner blood-retina barrier in the eye of Macaca mulatta. Invest Ophthalmol Vis Sci 1987; 28:2000-14.
53. Vinores SA, Derevjanik NL, Ozaki H, Okamoto N, Campochiaro PA. Cellular mechanisms of blood-retinal barrier dysfunction in macular edema. Doc Ophthalmol 1999; 97:217-28.
54. Behzadian MA, Windsor LJ, Ghaly N, Liou G, Tsai NT, Caldwell RB. VEGF-induced paracellular permeability in cultured endothelial cells involves urokinase and its receptor. FASEB J 2003; 17:752-4.
55. Mandriota SJ, Seghezzi G, Vassalli JD, Ferrara N, Wasi S, Mazzieri R, Mignatti P, Pepper MS. Vascular endothelial growth factor increases urokinase receptor expression in vascular endothelial cells. J Biol Chem 1995; 270:9709-16.
56. Kroll J, Waltenberger J. The vascular endothelial growth factor receptor KDR activates multiple signal transduction pathways in porcine aortic endothelial cells. J Biol Chem 1997; 272:32521-7.
57. Wu HM, Yuan Y, Zawieja DC, Tinsley J, Granger HJ. Role of phospholipase C, protein kinase C, and calcium in VEGF-induced venular hyperpermeability. Am J Physiol 1999; 276:H535-42.
58. Clancy RM, Rediske J, Tang X, Nijher N, Frenkel S, Philips M, Abramson SB. Outside-in signaling in the chondrocyte. Nitric oxide disrupts fibronectin-induced assembly of a subplasmalemmal actin/rho A/focal adhesion kinase signaling complex. J Clin Invest 1997; 100:1789-96.
59. Salzman AL, Menconi MJ, Unno N, Ezzell RM, Casey DM, Gonzalez PK, Fink MP. Nitric oxide dilates tight junctions and depletes ATP in cultured Caco-2BBe intestinal epithelial monolayers. Am J Physiol 1995; 268:G361-73.
60. Bacallao R, Garfinkel A, Monke S, Zampighi G, Mandel LJ. ATP depletion: a novel method to study junctional properties in epithelial tissues. I. Rearrangement of the actin cytoskeleton. J Cell Sci 1994; 107:3301-13.
61. Takeda M, Mori F, Yoshida A, Takamiya A, Nakagomi S, Sato E, Kiyama H. Constitutive nitric oxide synthase is associated with retinal vascular permeability in early diabetic rats. Diabetologia 2001; 44:1043-50.
62. Joussen AM, Poulaki V, Tsujikawa A, Qin W, Qaum T, Xu Q, Moromizato Y, Bursell SE, Wiegand SJ, Rudge J, Ioffe E, Yancopoulos GD, Adamis AP. Suppression of diabetic retinopathy with angiopoietin-1. Am J Pathol 2002; 160:1683-93.
63. Hirase T, Staddon JM, Saitou M, Ando-Akatsuka Y, Itoh M, Furuse M, Fujimoto K, Tsukita S, Rubin LL. Occludin as a possible determinant of tight junction permeability in endothelial cells. J Cell Sci 1997; 110:1603-13.
64. Kevil CG, Okayama N, Trocha SD, Kalogeris TJ, Coe LL, Specian RD, Davis CP, Alexander JS. Expression of zonula occludens and adherens junctional proteins in human venous and arterial endothelial cells: role of occludin in endothelial solute barriers. Microcirculation 1998; 5:197-210.
65. Kale G, Naren AP, Sheth P, Rao RK. Tyrosine phosphorylation of occludin attenuates its interactions with ZO-1, ZO-2, and ZO-3. Biochem Biophys Res Commun 2003; 302:324-9.
66. Spoerri PE, Robinson WG, Player D, Groome AB, Alexander T, Bodkin NL, Hansen BC, Grant MB. Diabetes related increase

in plasminogen activator inhibitor-1 expression in monkey retinal capillaries. Int J Diabetes 1998; 6:15-27.

67. Grant MB, Ellis EA, Caballero S, Mames RN. Plasminogen activator inhibitor-1 overexpression in nonproliferative diabetic retinopathy. Exp Eye Res 1996; 63:233-44.
68. Grant MB, Wargovich TJ, Bush DM, Player DW, Caballero S, Foegh M, Spoerri PE. Expression of IGF-1, IGF-1 receptor and TGF-beta following balloon angioplasty in atherosclerotic and normal rabbit iliac arteries: an immunocytochemical study. Regul Pept 1999; 79:47-53.
69. Grant MB, Afzal A, Spoerri P, Pan H, Shaw LC, Mames RN. The role of growth factors in the pathogenesis of diabetic retinopathy. Expert Opin Investig Drugs 2004; 13:1275-93.

The print version of this article was created on 12 Jan 2006. This reflects all typographical corrections and errata to the article through that date. Details of any changes may be found in the online version of the article.